International Forum on Aeroelasticity and Structural Dynamics
IFASD 2024
17-21 June 2024, The Hague, The Netherlands

AEROELASTIC OPTIMIZATION OF LARGE AIRCRAFT CONSIDERING HIGH PRECISION AERODYNAMIC

Keyu Li[1], Chao Yang[1], Xiaozhe Wang[*,2], Zhiqiang Wan[1], Liang Ma[1] and Chang Li[1]

1 School of Aeronautic Science and Engineering, Beihang University , Beijing 100191, China;
2 Institute of Unmanned System, Beihang University , Beijing 100191, China

Keywords: Commercial aircraft, Aeroelastic tailoring, Kriging surrogate model

Abstract: During the design stage of commercial aircraft, aeroelastic tailoring can efficiently improve the wing's aeroelastic properties. However, the high-precision aerodynamic analysis method used in static aeroelastic analysis is time-consuming and not suitable for tailoring design. This paper proposes an aeroelastic optimization method that considers high-precision aerodynamics. The wing torsion angle and deflection are used to realize a high-precision aeroelastic prediction through the Kriging surrogate model. Additionally, a genetic algorithm is employed to optimize the wing skin and web layup thickness variables while considering stiffness, strength, aerodynamic, and aileron efficiency constraints. The objective is to minimize the structural mass of the wing. The results indicate that the surrogate model error is 0.32%, which realizes the efficient prediction of aerodynamic. Furthermore, the final wing configuration achieves a 20 kg reduction in mass compared to the initial configuration while satisfying the constraints.

1 INTRODUCTION

Modern large aircraft usually employ composite wings with high aspect ratios, which have significant bending and torsional coupling characteristics and aeroelastic effects[1]. The conventional approach to solve the aeroelasticity problem is to minimize the structural deformation by enhancing the structural stiffness. However, this method results in increased structural weight and reduced overall aircraft performance[2]. Therefore, modern design concepts propose fully considering the effect of aeroelasticity during the aircraft design stage and maximizing the use of structural deformation through aeroelasticity optimization to enhance the aircraft's aerodynamic characteristics[3].

In the context of commercial aircraft, which are distinguished by their large aspect ratios, it can be observed that they exhibit significant aeroelastic properties. Therefore, it is essential to consider the effect of elastic deformation on aerodynamic forces in the design process through the application of aerodynamic-structural coupling techniques[4]. Aeroelastic entails the development of analysis methods, simulation models, design schemes, and optimization methods that are applicable to each design stage, according to the design characteristics and requirements of the conceptual, preliminary, and detailed design stages in the aircraft design process. For instance, in the preliminary stage, a two-dimensional panel beam structure and a three-dimensional aerodynamic surface are employed to determine the aerodynamic shape, the front and rear spar

positions, and the structural dimensions of the wing through optimization[5]. The static aeroelastic deformation of the wing is controlled through the tailoring design, ensuring that the airplane can achieve the desired comprehensive performance. Sachin et al.[6] used an aeroelastic optimization approach to reduce the weight of the wing structure while ensuring that the composite wing meets the strength, stiffness and flutter design requirements. Brooks[7]used a adjoint approach to develop an aerodynamic/structural optimization design framework with a large number of design variables for a large aspect ratio wing. Once the aerodynamic shape of the wing and the structural arrangement of the wing have been determined, in order to address the aeroelasticity problem, it is necessary to evaluate the specific influence of the structural sizes on the aerodynamic characteristics of the cruising state. At this stage of the optimization process, the linear method to calculate aerodynamic forces is often employed[8]. However, the method is unable to accurately assess the drag, and the high-precision calculation method often requires a significant amount of time for aerodynamic calculation, which is not conducive to the efficiency of optimization.

This paper presents a study of the tailoring design framework for the deepening stage of the large aircraft. In order to enhance computational efficiency while maintaining computational accuracy, an aeroelastic optimization framework based on the surrogate model is proposed for the purpose of realizing the wing tailoring, taking into account both the aeroelasticity and the high-precision aerodynamic performance constraints.

2 METHODS

2.1 Aerodynamic

Large aircraft typically cruise at high subsonic speeds, during which shock waves occur. The aerodynamic drag must take into account the effect of the shock wave drag. Euler theory is applicable to flight conditions involving complex-shaped vehicle and large angle of approach. It can effectively calculate induced drag and shock wave drag. Therefore, this paper utilizes Euler theory to solve for the aerodynamic force. The integral form of the theory is expressed as follows:

$$\frac{\partial}{\partial t}\iiint_{V}\boldsymbol{F}\mathrm{d}V+\iint_{\partial V}\boldsymbol{E}\cdot\hat{\boldsymbol{n}}dS=0 \tag{1}$$

$$\begin{cases}\boldsymbol{F}=\begin{bmatrix}\rho & \rho u & \rho v & \rho w & \rho e\end{bmatrix}^{\mathrm{T}}\\ \boldsymbol{E}=\begin{bmatrix}\rho u\boldsymbol{i}+\rho v\boldsymbol{j}+\rho w\boldsymbol{k}\\ (\rho u^2+p)\boldsymbol{i}+\rho uv\boldsymbol{j}+\rho uw\boldsymbol{k}\\ \rho uv\boldsymbol{i}+(\rho v^2+p)\boldsymbol{j}+\rho vw\boldsymbol{k}\\ \rho uw\boldsymbol{i}+\rho vw\boldsymbol{j}+(\rho w^2+p)\boldsymbol{k}\\ \rho hu\boldsymbol{i}+\rho hv\boldsymbol{j}+\rho hw\boldsymbol{k}\end{bmatrix}\end{cases} \tag{2}$$

where $\boldsymbol{F}$ is the conservation vector, $\boldsymbol{E}$ is the stream vector flux, ∂V is the boundary of a fixed region V, ρ is the density of air, e is the internal energy per unit mass of gas, $\hat{\boldsymbol{n}}$ is the outer normal vector of the boundary, h is the total enthalpy. Euler theory does not account for viscous effects; therefore, viscous corrections to the drag are necessary. The correction can be achieved by calculating the boundary layer integral along the surface flow line. This correction is an iterative process that typically requires three to five viscous/non-viscous cycles.

2.2 Static aeroelastic analysis

Aeroelastic static problems are of two main types: the first is the torsional divergence problem and the closely related load redistribution problem; the second is the maneuvering efficiency and maneuvering backlash problem. Currently, the primary aerodynamic methods used for aeroelastic analysis are linear and nonlinear aerodynamic methods. Linearized aerodynamic potential flow theory is a quick method for providing preliminary aerodynamic loads for engineering applications. However, in cases where the nonlinear behavior of aerodynamic forces is significant, the N-S equation or Euler's equation must be used for aerodynamic solutions. Aeroelastic coupling methods based on nonlinear aerodynamic forces include two types: loose coupling and tight coupling. The loose-coupling method has the advantage of requiring less computational power and achieving better convergence than the tight-coupling method. The finite element method is used to solve the structure. The data exchange between the structural and aerodynamic models is accomplished through the shape function and surface spline interpolation methods. The flow chart is shown in Fig.1.

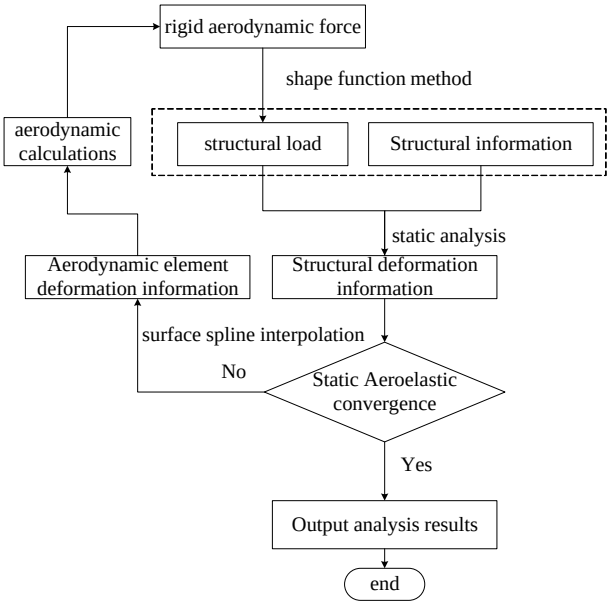

Fig.1 Flow chart of static aeroelastic analysis

2.3 Maneuvering efficiency

The maneuvering efficiency problem typically refers to the effect of the elastic deformation of the lifting surface structure on the efficiency of the rudder surface, which is mostly seen in the aileron. As flight speed increases, the airfoil structure's elastic deformation also increases, resulting in a reduction in rudder maneuvering efficiency. Aileron efficiency is defined as:

$$\eta = \left(\partial C_{mx} / \partial \delta_a\right)_e / \left(\partial C_{mx} / \partial \delta_a\right)_r \tag{3}$$

where C_{mx} is the aircraft roll moment coefficient, δ_a is the aileron deflection, the subscript e denotes elasticity, and the subscript r denotes rigid.

2.4 Failure guidelines for laminates

The failure criterion is a crucial strength constraint in the optimal design of composite laminates. The commonly used failure criterion is the Tsai–Wu failure criterion, the expression of which simplifies to for the plane stress state:

$$F_{11}\sigma_1^{\ 2} + 2F_{12}\sigma_1\sigma_2 + F_{22}\sigma_2^{\ 2} + F_{66}\sigma_6^{\ 2} + F_1\sigma_1 + F_2\sigma_2 = 1 \tag{4}$$

where:

$$F_1 = \frac{1}{X_t} - \frac{1}{X_c}, F_1 = \frac{1}{Y_t} - \frac{1}{Y_c}, F_{12} = 0 \tag{5}$$

$$F_{11} = \frac{1}{X_t X_c}, F_{22} = \frac{1}{Y_t Y_c}, F_{66} = \frac{1}{Y_S^{\ 2}} \tag{6}$$

Where X_t, X_c are longitudinal tensile and compressive strength, Y_t, Y_c are transverse tensile and compressive strength, and Y_S is the shear strength.

3 AEROELASTIC TAILORING OF LARGE AIRCRAFT CONSIDERING HIGH-PRECISION AERODYNAMIC PERFORMANCE CONSTRAINT BASED ON THE KRIGING SURROGATE METHOD

3.1 Optimization model

The optimization study in aeroelasticity is a standard problem that involves searching for a set of design variables in *ndv*-dimensional space to minimize the objective function.

$$\begin{aligned} &Min && F(v) && \\ &S.T. && g_j(v) \le 0 && j = 1,2,...,ncon \\ &v_i^{lower} \le v_i \le v_i^{upper} && && i = 1,2,...,ndv \end{aligned} \tag{7}$$

where, $F(v)$ is the objective function; $g(v)$ is used to specify the inequality constraints, such as deformation constraints, strength constraints, aileron efficiency constraints, etc, v_i is used to specify the upper and lower limits of the design variables, also known as boundary constraints.

3.2 Design variable

The wing skin's structural parameters, as well as those of the front and rear beam webs, are determined during the detailed design stage. The thickness increases at the inner wing section and decreases at the outer wing section along the span. Fig.2 shows a total of 137 structural parameters. The range of structural design variables is between 2 and 15 mm.

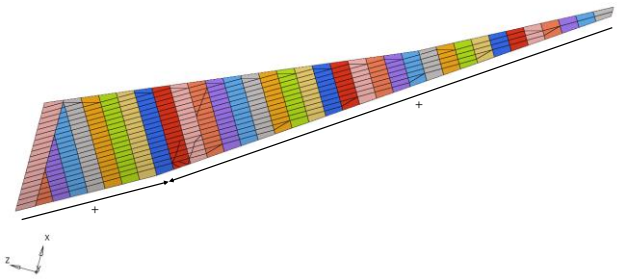

Fig.2 Design variables

3.3 Constraint

The constraints include strength constraint, deformation constraint, lift efficiency constraint, aileron efficiency constraint, and aerodynamic performance constraint. Specific parameters are shown in the Table 1.

Table 1 Structural response and scope of constraint

Structural response		Scope of constraint
Strength constraint	Spar stress(Mpa)	[-260,358]
	Beam flange stress(Mpa)	[-260,358]
	Failure constraint (Cai-Hu tensor criterion)	[-1,1]
Deformation constraint	Wingtip displacement(mm)	≤ 1800 (6% of half span length)
	Wingtip torsion angle(°)	≤ 3
Lift efficiency constraint	Lift curve slope	[5,6]
Aileron efficiency constraint	Aileron efficiency	$\geq 60\%$
Aerodynamic performance constraint	Lift-drag ratio	[15.52,17.0]

The aerodynamic model is shown in Fig.3. The baseline cruise profile has a lift-to-drag ratio of 15.52 after viscous/non-viscous iterations.

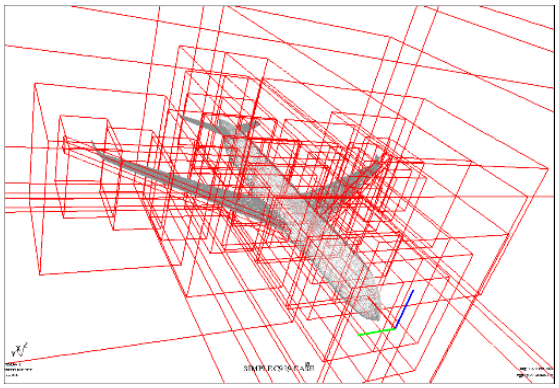

Fig.3 Aerodynamic model

The lift and drag characteristics of an elastic wing are primarily determined by the bending and torsional deformation of the wing in the spreading direction. The bending and torsional deformations are shown schematically in Fig.4.

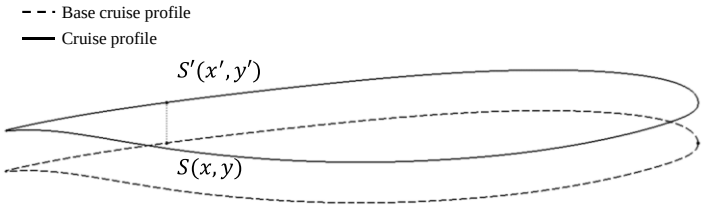

(a) Bending deformation

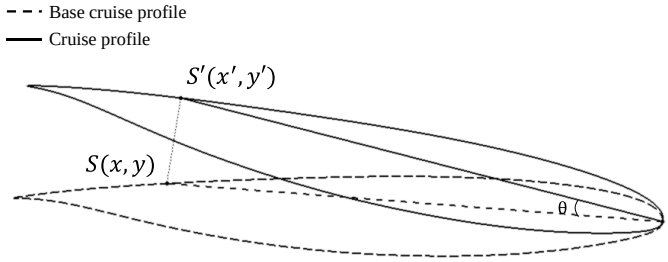

(b) torsional deformation

Fig.4 primarily deformation of the wing

The Kriging surrogate modeling is a linear regression method that ensures the response function passes through all sample points. The prediction function comprises a linear regression and a stochastic function. For a problem with q response conditions, the prediction function for the lth response is expressed as:

$$y_l(x) = f_l(x) + z_l(x) \qquad l = 1, 2, ..., q \tag{8}$$

where x is an n-dimensional vector, $f_l(x)$ is the regression model, $z_l(x)$ is a stochastic function based on sample statistics. In this paper, the regression model is a first-order polynomial and the stochastic model is a Gauss function.

Therefore, the inputs to the surrogate model are the wing's leading edge point coordinates and torsion angles in different profiles in the spreading direction.

3.4 Optimisation strategy

The design problem for aeroelastic tailoring in composite wing involves determining the optimal composite wing skin and web layup thicknesses to achieve the lightest structural weight while satisfying constraints for deformation, strength, aerodynamic conductivity, and aerodynamic performance.The flow chart is shown in Fig.5.

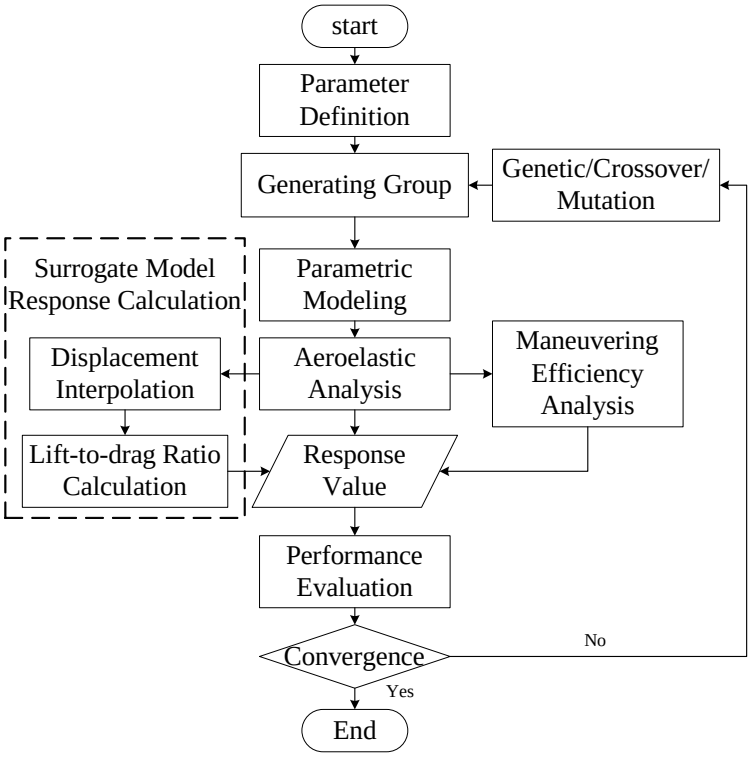

Fig.5 Optimization framework flowchart

This hybrid algorithm combines the genetic algorithm for global search with the modified feasible direction method for local optimization. The genetic algorithm prevents the algorithm from getting stuck in local optimized solutions, while the modified feasible direction method further optimizes the good individuals obtained from the genetic algorithm. This approach allows for the gradual convergence of global optimized solutions through repeated search.

The calculation of the response to constraints such as deformation, stress, and maneuvering efficiency is performed through aeroelasticity analysis. The static aeroelastic results obtained based on linear aerodynamic are in general agreement with the nonlinear aerodynamic results. Therefore, the deformation, strength and aerodynamic derivative responses of the optimisation problem are obtained by the static aeroelastic analysis method based on linear aerodynamic. This improves the efficiency of the optimisation process. The aerodynamic performance response could be calculated using Euler's theory. This is because the accurate drag coefficient cannot be obtained by the linearized aerodynamic potential flow theory. However, including computational fluid dynamics (CFD) analysis in the aeroelastic tailoring process will result in a significant increase in computational cost. This paper employs the Kriging surrogate model to calculate the lift-to-drag ratio of the entire airplane.

4 RESULT

4.1 Prediction of aerodynamic performance response based on Kriging surrogate model

The flight speed corresponds to 0.85Ma and the required lift coefficient is 0.48. In order to validate the accuracy of the Kriging surrogate model for this algorithm, the torsion angle and leading edge displacement of the 38 airfoils of the selected cruise profile were input to obtain the full-aircraft lift-to-drag ratio response, as illustrated in Fig.6. The Kriging surrogate model was trained using 803 samples, and subsequently validated by 6 samples.

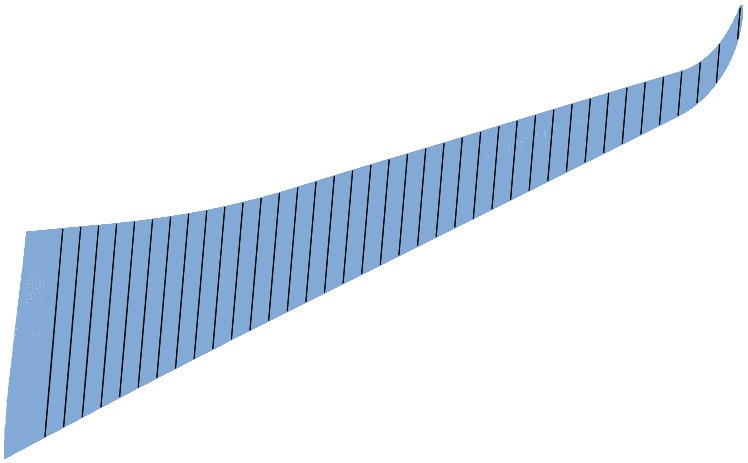

Fig.6 Airfoils of the cruise profile along the span

The errors between the surrogate model response values and the true values are shown in Table2. The average relative error of the aerodynamic lift-drag ratio is 0.32%, with the maximum relative error being within 1%. The surrogate model's accuracy meets the requisite standards and can be employed for the prediction of the response lift-drag ratio constraint in the optimised design.

Table2 The results of CFD and surrogate model

	lift-drag ratio(CFD)	lift-drag ratio(surrogate model)	relative error
Sample 1	15.1080	15.1205	0.08%
Sample 2	15.1272	15.1359	0.06%
Sample 3	15.4803	15.4677	0.08%
Sample 4	15.1954	15.2389	0.29%
Sample 5	15.0412	15.1837	0.95%
Sample 6	15.1410	15.0695	0.47%

4.2 Aeroelastic optimization of aircraft considering high precision aerodynamic

This paper presents a finite element model based on the wing geometry of a typical large aircraft. The aircraft's upper and lower wing skins, wing ribs, and front and rear beam webs are modeled using plate elements. The front and rear beam flanges, upper and lower trusses use rod elements. The finite element model of the aileron and other control surfaces use beam elements. The engine is simulated using a centralized mass, which is connected to the wing through a beam element. The initial configuration wing has a mass of 34,260 kg.

The optimised individual was obtained by genetic optimisation algorithm. The relative thicknesses of the composite wing upper and lower skins, front and rear webs layups before and after optimisation are shown in Fig.7-Fig.10. The blue columns are the parameters of the initial configuration and the red columns are the parameters of the optimised design configuration. The maximum thicknesses of the initial configuration and the optimised design configuration in the region are taken as the reference thicknesses, and the thicknesses of the layups are normalised. The closer relative thickness is to 1, the greater the thickness is indicated. For ease of description, within 40% of the half-spread length is defined as the inner section of the wing, between 40% and

80% of the half-spread length is defined as the middle section of the wing, and beyond 80% is defined as the outer section of the wing. The optimisation of the upper skin and rear beam web layup resulted in a similar reduction in the thickness of the inner and middle sections of the wing, while the outer section of the wing was thickened. The thickness of the lower skin and front beam web is primarily increased in the middle and outer sections.

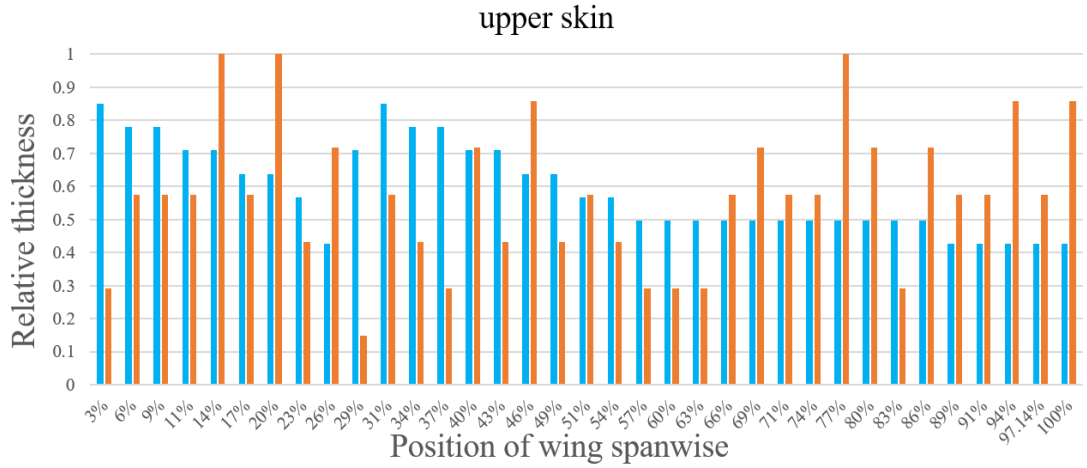

Fig.7 Relative thickness of upper skin

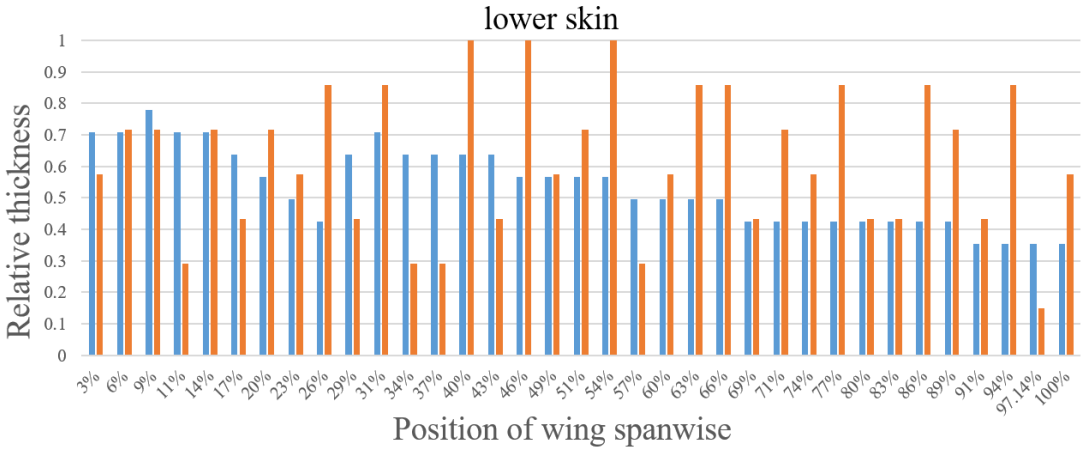

Fig.8 Relative thickness of lower skin

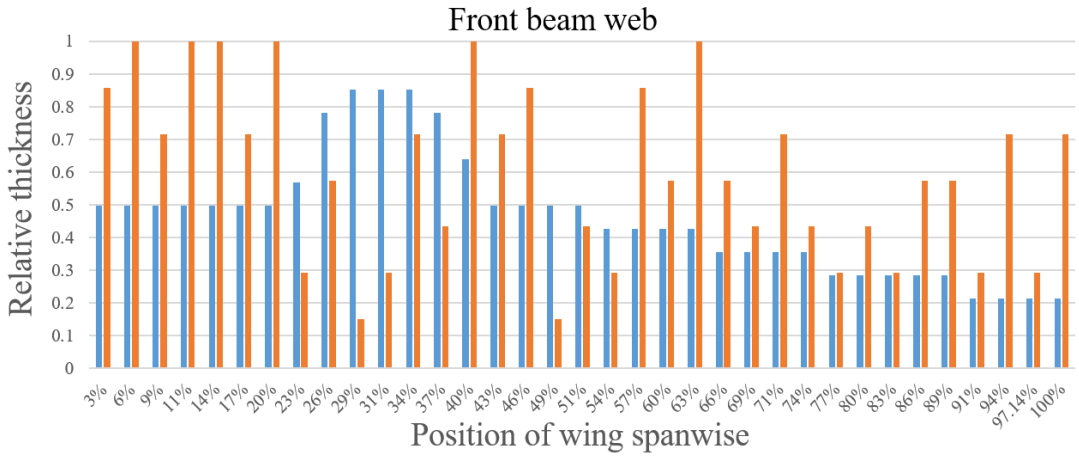

Fig.9 Relative thickness of front beam web

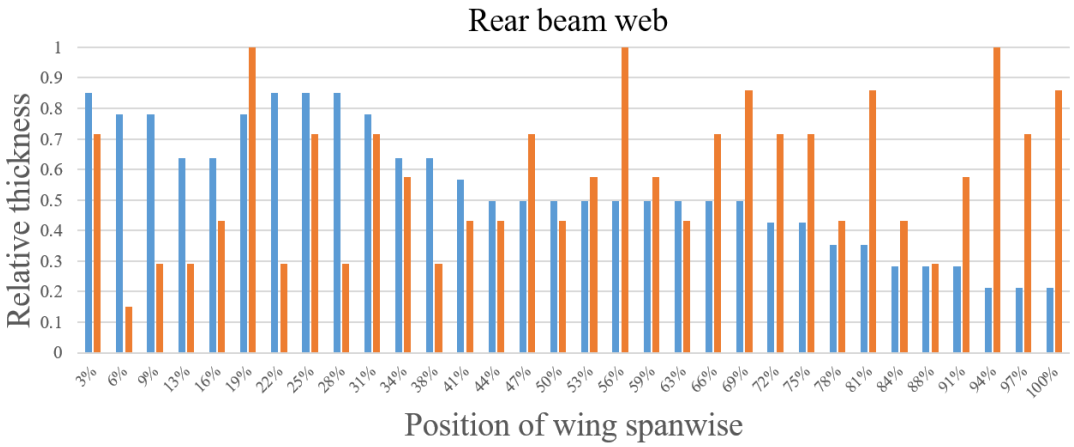

Fig.10 Relative thickness of rear beam web

The final design configuration exhibits a mass reduction of 20 kg, contingent upon the simultaneous satisfaction of all static aeroelastic constraints. Furthermore, the lift-to-drag ratio of 15.67 is obtained from the CFD/CSD coupled calculation of the final design wing configuration, which is verified to meet the requirements of aerodynamic performance. This also demonstrates the efficacy of the aeroelastic optimisation methodology based on the surrogate model. Table3 presents a comparison between the constraints of the optimal design configuration and the initial configuration. The example model exhibits a considerable margin in deformation constraints, lift efficiency constraints, and aileron efficiency constraints. The initial configuration exhibits a superior aerodynamic configuration, thereby rendering the aerodynamic lift-to-drag ratio the most critical constraint in determining the optimisation.

Table3 The constraints of the optimal design and the initial configuration

Structural response	Scope of constraint	The initial configuration	The optimal design configuration
Wing mass(t)		34.26	34.24
Wingtip displacement(mm)	⩽1800	743.18	829.74
Wingtip torsion angle(°)	⩽3	-0.173	-0.215
Lift efficiency	[5,6]	5.370	5.381
Aileron efficiency	⩾0.6	0.729	0.718
Lift-to-drag ratio	[15.52,17.0]	15.52	15.67

The variation of deflection and torsion angle along the spanwise direction for the cruise profile of the initial and optimised configurations of this algorithm is presented in Fig.11,Fig.12. The aerodynamic performance changes of the swept-back wing are primarily attributable to the negative twist and the bending deformation along the spreading direction, which are a consequence of aeroelasticity. A reduction in the effective angle of the wing due to negative torsion results in a decline in both the lift and drag coefficients. The bending deformation results in the loss of aerodynamic force in the vertical direction, which in turn leads to a decrease in the lift coefficient

and induced drag. The elastic deformation of the swept-back wing results in a reduction in the lift-to-drag ratio. However, through the optimal design of wing aeroelasticity, which considers the aerodynamic performance constraints, the thickness of the wing layup along the spreading direction can be reasonably allocated for the stiffness design. This allows for the creation of a better configuration with no degradation of aerodynamic performance, while reducing the weight of the wing structure.

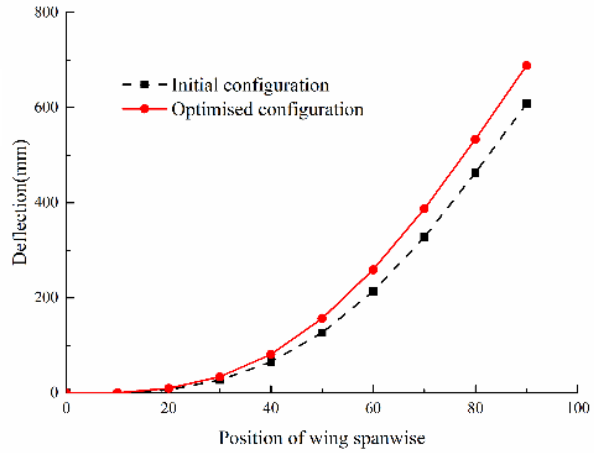

Fig.11 Deflection of initial configuration and optimized configuration

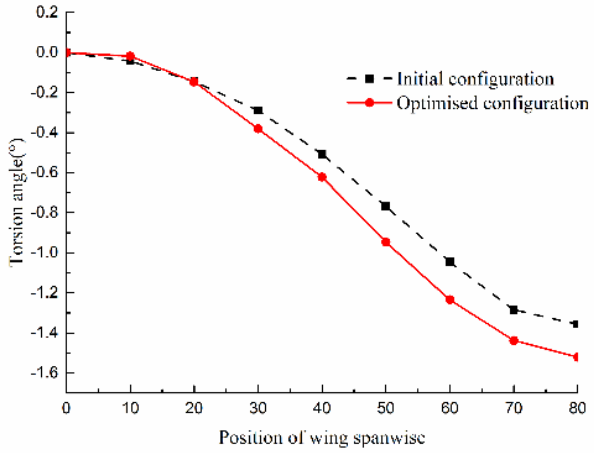

Fig.12 Torsion angle of initial configuration and optimized configuration

The pressure coefficient distributions for different spreading profiles are presented in Fig.13 . The initial configuration_20% indicates the pressure coefficient distribution at 20% of the wing spread direction for the initial configuration. The pressure coefficient distributions of the initial configuration and the optimised configuration at the inner section of the wing (20%, 40%) are not significantly different. This is due to the fact that the bending and torsional deformations in the inner section of the wing are minimal, resulting in a relatively unchanged aerodynamic performance of the inner section of the wing for the cruise profile. The optimised configuration exhibits a slightly elevated lift coefficient in the middle section of the wing (60%) in comparison to the initial configuration, while it exhibits a slightly reduced lift coefficient in the outer section of the wing (80%).

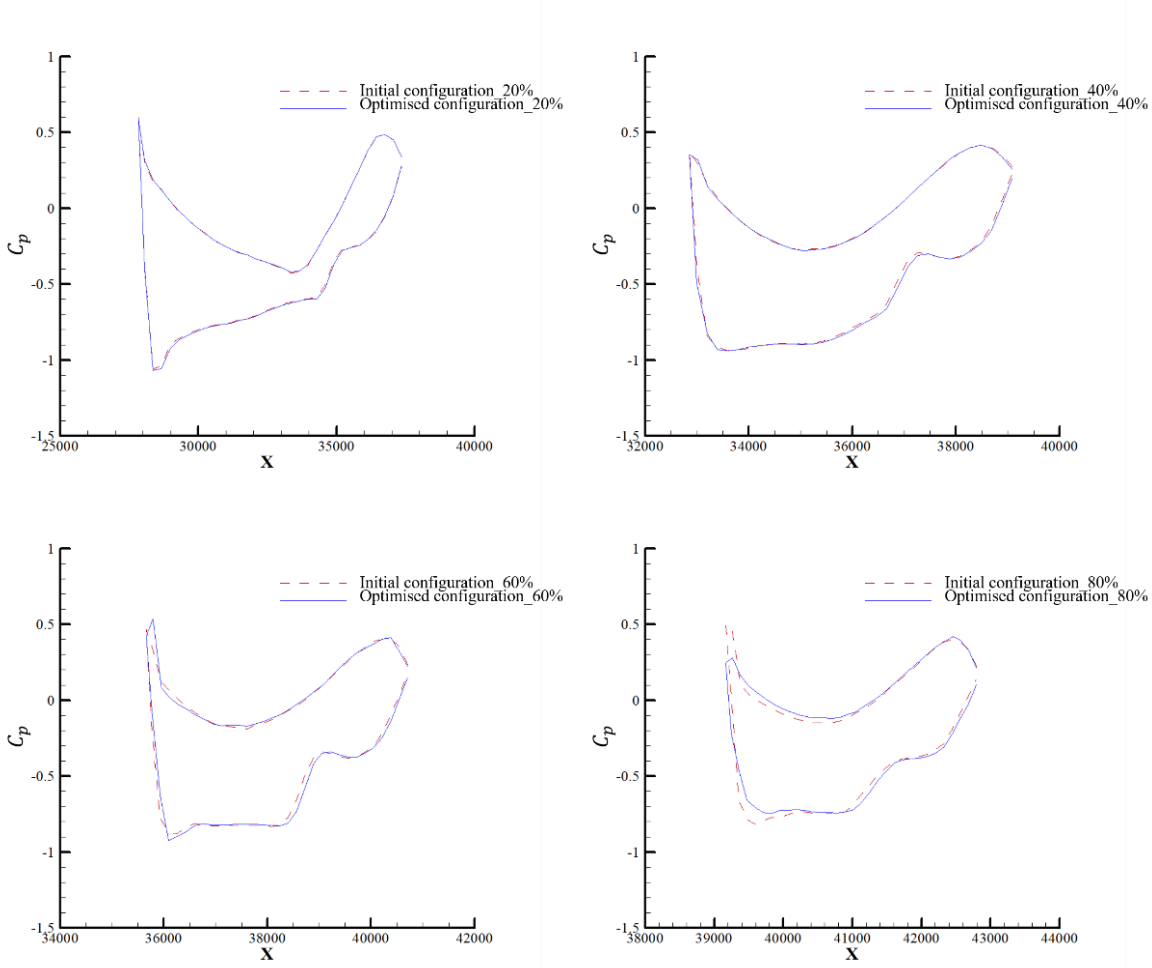

Fig.13 The pressure coefficient distributions for different spreading profiles

5 CONCLUSIONS

This paper presents a methodology for the aeroelastic tailoring of large aircraft considering high-precision aerodynamic performance constraint based on the Kriging surrogate method. The principal findings are as follows:

(1) In terms of aerodynamic performance prediction, the application of an surrogate model can efficiently achieve aerodynamic response prediction and improve the optimisation efficiency.

(2) At the detailed design stage, the tailoring design of large aircraft is carried out by the aeroelastic optimisation method based on the Kriging surrogate model. This method allows for the reduction of structural weight of the wing while ensuring compliance with aeroelastic constraints and maintaining optimal aerodynamic performance.

REFERENCES

[1] KILIMTZIDIS S, KOSTOPOULOS V. Static aeroelastic optimization of high-aspect-ratio composite aircraft wings via surrogate modeling[J]. Aerospace, 2023, 10(3).

[2] WANG X, WAN Z, LIU Z, et al. Integrated optimization on aerodynamics-structure coupling and flight stability of a large airplane in preliminary design[J]. Chinese Journal of Aeronautics, 2018, 31(6): 1258-1272.

[3] KAFKAS A, KILIMTZIDIS S, KOTZAKOLIOS A, et al. Multi-fidelity optimization of a composite airliner wing subject to structural and aeroelastic constraints[J]. Aerospace, 2021, 8(12).

[4] KILIMTZIDIS S, KOSTOPOULOS V. Multidisciplinary structural optimization of novel high-aspect ratio composite aircraft wings[J]. Structural and Multidisciplinary Optimization, 2023, 66(7).

[5] WAN Z, LIU D, TANG C, et al. Studies on the influence of spar position on aeroelastic optimization of a large aircraft wing[J]. Science China Technological Sciences, 2011, 55(1): 117-124.

[6] SHRIVASTAVA S, TILALA H, MOHITE P M, et al. Weight optimization of a composite wing-panel with flutter stability constraints by ply-drop[J]. Structural and Multidisciplinary Optimization, 2020, 62(4): 2181-2195.

[7] BROOKS T R, MARTINS J R R A, KENNEDY G J. Aerostructural tradeoffs for tow-steered composite wings[J]. Journal of Aircraft, 2020, 57(5): 787-799.

[8] CROVATO A, ALMEIDA H S, VIO G, et al. Effect of levels of fidelity on steady aerodynamic and static aeroelastic computations[J]. Aerospace, 2020, 7(4).

COPYRIGHT STATEMENT

The authors confirm that they, and/or their company or organisation, hold copyright on all of the original material included in this paper. The authors also confirm that they have obtained permission from the copyright holder of any third-party material included in this paper to publish it as part of their paper. The authors confirm that they give permission, or have obtained permission from the copyright holder of this paper, for the publication and public distribution of this paper as part of the IFASD 2024 proceedings or as individual off-prints from the proceedings.